

REPORT ON PHASE 6 CAUSAL MODELING FOR SCHIPHOL AIRPORT

O Morales, D Kurowicka, R Cooke, I Jagielska
EWI, TU Delft,
May, 2007

1. INTRODUCTION.

This document reports on the activities of EWI during the sixth phase of the CATS project; that is, the time period between the end of February 2007 and the end of June 2007. The project kicked off in July 2005, although preparatory work was initiated in the spring of the same year.

The previous report [12] described an overview of the progress in the work being done to translate ESDs & FTs into BBNs and a preliminary suggestion on how to connect continuous BBNs to each ESD & FT once they have been written as BBNs.

In this report we present:

- A first quantification of the Air Traffic Control Human Performance Model.
- UniExp: software tool for the elicitation of conditional rank correlations as input for Distribution Free Discrete/Continuous BBNs,
- UniExp's users manual.

2. AIR TRAFFIC CONTROL HUMAN PERFORMANCE MODEL.

Meetings have been held from December 19th 2006 to March 1st 2007 between personnel from NLR and TU-Delft for building up the causal model. It was decided that the Flight Crew Performance Model presented in [4] and [6] would be a starting point for the construction of the model. The BBN representing the model is presented in Figure 1. As usual nodes in the BBN represent random variables and arcs unconditional and conditional rank correlations between them. The six rank correlations in Figure 1 were elicited in a dry run exercise from a single air traffic controller in order to test our elicitation instrument. Variable 7 "*Time of Day*" was excluded from this exercise but might be incorporated in future versions of the model.

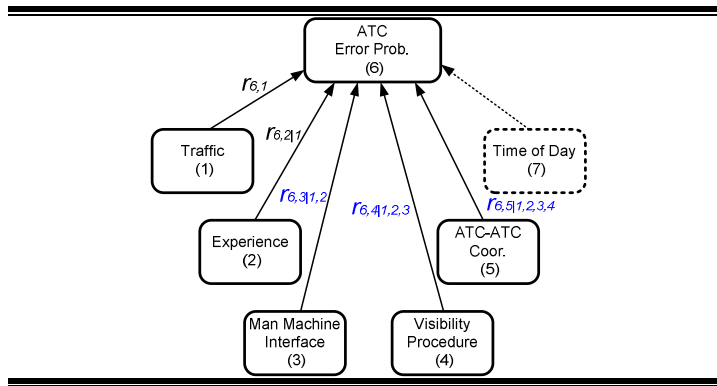


Figure 1. Air Traffic Control Error Probability Model

2.1 MARGINAL DISTRIBUTIONS.

The marginal distributions of the 6 variables entering the model in this report were obtained from data by NLR¹. Information about these variables is summarized in Table 1. Variables 1, 2 and 6 are approximated by continuous distributions whereas variables 3, 4, and 5 are discrete.

2.1.1. ATC ERROR PROBABILITIES.

The ATC error probability is a base event in the FTs built by DNV. A list of events influenced by ATC human performance is presented in appendix 1. In general, confidence bands are computed for each probability presented in appendix 1 and a minimally informative distribution is fitted to the data assuming the 3 point estimates represent the 5th 50th and 95th percentiles of a continuous distribution.

2.1.2. TRAFFIC.

The distribution of traffic, defined as the number of aircraft simultaneously under control of a single ATCo, is based on Eurocontrol Central Flow Management Unit (CFMU) data of four days of movements into the Schiphol ACC sector via one of the three entries. The data lists the number of aircraft per time frame of one hour that entered the sector.

Using estimates for the size of the airspace and the average speed of the aircraft, the average time of an aircraft in the sector as well as the number of aircraft simultaneously in the sector can be computed. With an airspace size of 100 km and an average speed of 350 kts, the average time of an aircraft in the airspace is 9.3 minutes. If, e.g., there are 3 aircraft per hour entering the sector via one entry (based on the CFMU data), in total there are 9 aircraft per hour in the airspace, which comes down to an estimated $9 \cdot 9.3 / 60 = 1.39$ aircraft simultaneously under control. The resulting distribution is shown in Figure 2 (a).

¹ In the case of ATC error probability, the distribution comes from fitting a minimally informative distribution with respect to the log uniform measure to data obtained by DNV.

Node	Definition	Unit	Source for marginal distribution
ATC Error Probability	Number of air traffic control errors per demand	Number of errors	DNV aoult tree quantification reports
Traffic	Number of aircraft simultaneously under control by ATCo	Number of aircraft	CTFM/FTFM data
Experience	Number of years working as an ATCo at current position	number of years	Eurocontrol report on Age, Experience and Automation in European ATC – Survey in the ECAC area
Man Machine Interface (MMint)	Classification of the interface that is used by the ATCo. Four classes are distinguished, based on the availability of supporting systems: 1. radio only 2. radio and primary radar 3. radio and primary and secondary radar 4. radio and primary and secondary radar and additional tools (e.g. RIASS, STCA)	1 – 4	Survey of European airports
Visibility procedure (Vis_Proc)	Current visibility procedure in use, distinguishing: 1. normal operations: RVR above 1500m and cloud base above 300ft. 2. BZO A: RVR between 550m and 1500m or cloud base between 200ft and 300ft (associated with Cat I) 3. BZO B: RVR between 350m and 550m or cloud base below 200ft (associated with Cat II) 4. BZO C: RVR between 200m and 350m (associated with Cat 3A) 5. BZO D: RVR below 200m (associated with Cat 3B) BZO A – D are in place at Schiphol airport. BZO stands for 'Bijzondere Zicht Operatie' (Limited Visibility Operations). RVR stands for Runway Visual Range.	1 – 5	Schiphol operational and/or meteorological data
ATC co-ordination (Coordin)	Whether or not the co-ordination between ATCo's takes place in the same room or not. (without or with the use of telephone/radio)	yes/no	

Table 1. Definitions of variables from Figure 1.

Note that this distribution is based on only a relatively small set of data representing Schiphol ACC sector. In view of a lack of additional and more precise information, this distribution is assumed to be representative for the number of aircraft under control by ACC, APP, and TWR ATCO.

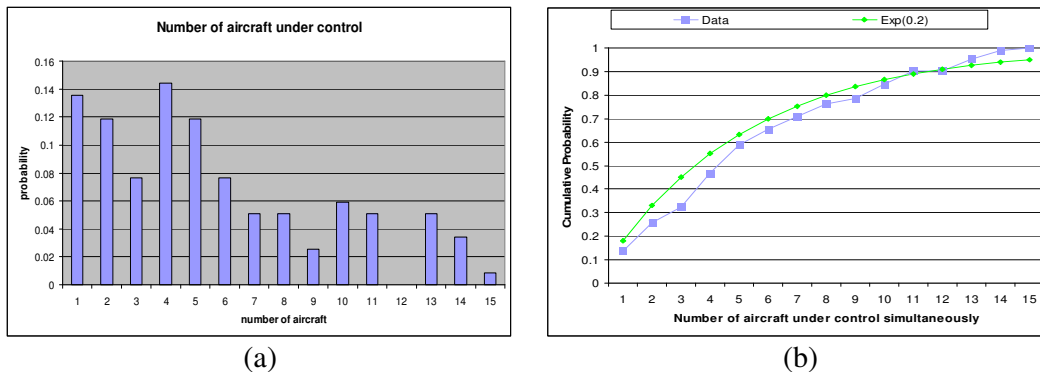


Figure 2. Number of Aircraft Simultaneously Under Control

In figure 2 (b) the cumulative probability is computed from figure 2 (a) and plotted together with an exponential distribution with parameter 0.2. This distribution has mean 5 and 5th and 95th percentiles 0.256466 and 14.97866 respectively. The exponential distribution will be used to approximate the distribution from figure 2 (a).

2.1.3. EXPERIENCE.

Data on experience of ATCO's is obtained from a Eurocontrol survey on age, experience, and automation in European ATC in the ECAC area. The distribution for the experience on the current positions is presented in Figure 3 (a) below. 1079 ATCOs from 28 countries participated in the survey. The average age of the subjects was 38,17 years, with a standard deviation (std) of 8,94. The youngest controller in the sample was 21 years old at the time of the survey, the oldest controller was sixty.

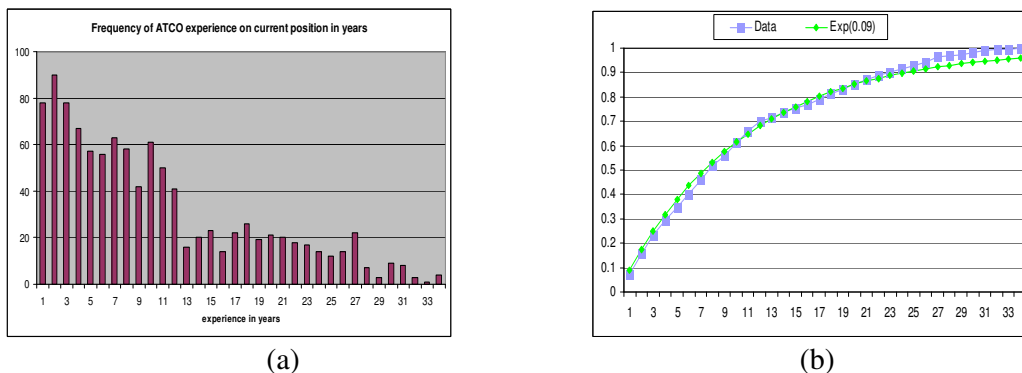


Figure 3. Number of Aircraft Simultaneously Under Control

The cumulative distribution function corresponding to figure 3 (a) is plotted together with an exponential distribution with mean value 10.5 in figure 3 (b). This continuous distribution will be used to approximate the distribution from figure 3 (a).

2.1.4. MAN MACHINE INTERFACE.

To quantify the influence of the MMI on ATCO performance, it is proposed to distinguish four classes of the MMI, based on the availability of supporting systems:

1. radio only,
2. radio and primary radar,
3. radio and primary and secondary radar, and
4. radio and primary and secondary radar and additional tools (e.g. A-SMGCS, STCA).

In Eurocontrol's 2005 status report on the European Convergence and Implementation Plan (ECIP), it is shown that about 80% of aircraft movements within the ECAC ACC's are supported by STCA. This number is taken as a representative for class 4 probability for ACC and APP controllers. It is furthermore noted in e.g. Eurocontrol's Surveillance Strategy for ECAC that Secondary Surveillance Radar (SSR) is widely implemented throughout the ECAC area. As 'widely' is not further specified, we assume that this refers to 99% of the ECAC area. If we further assume that class 1 'radio only' only can occur due to a radar failure and that this occurs with a probability 1 out of 10,000 movements, we obtain the following probabilities for the four classes:

Class	Probability of occurrence for ACC and APP
radio only	0.0001
radio and primary radar	0.0999
radio and primary and secondary radar	0.1900
radio and primary and secondary radar and additional tools (e.g. A-SMGCS, STCA).	0.8000

Table 2 Probability of occurrence for ACC and APP controllers

For TWR and GND controllers it is more appropriate to look at implementation of A-SMGCS (Advanced Surface Movement Guidance & Control System) Level 1 We then obtain the following probabilities for the four classes:

Class	Probability of occurrence for TWR and GND
radio only	0.0001
radio and primary radar	0.0999
radio and primary and secondary radar	0.7800
radio and primary and secondary radar and additional tools (e.g. A-SMGCS, STCA).	0.2100

Table 3 Probability of occurrence for TWR and GND controllers

2.1.5. VISIBILITY PROCEDURE.

For visibility, five classes are distinguished:

1. normal operations: Runway visual range (RVR) above 1500m and cloud base above 300ft.
2. BZO A: RVR between 550m and 1500m or cloud base between 200ft and 300ft (associated with Cat I)
3. BZO B: RVR between 350m and 550m or cloud base between 100ft and 200ft (associated with Cat II)
4. BZO C: RVR between 200m and 350m (associated with Cat 3A)
5. BZO D: RVR below 200m (associated with Cat 3B)

A graphical representation of these classes is given below.

300 ft < cloud base	N/A			2	1
200 < cloud base < 300ft	2				
100 < cloud base < 200ft	3		3		N/A
cloud base < 100ft	5	4			N/A
	RVR < 200m	200 < RVR < 350m	350 < RVR < 550m	550 < RVR < 1500m	RVR > 1500m

Figure 4 Graphical representation of visibility classes

Currently, only data on visibility is available. As, logically, there is correlation between RVR and cloud base, we therefore use these data on visibility only to estimate the probabilities of occurrence of the five classes. The available data set consists of about 27 million observations. Based on these data, the following probabilities are estimated.

Class	1	2	3	4	5
Probability	0.9587	0.0224	0.0048	0.0033	0.0107

Table 4 Probability of occurrence per visibility class

2.1.6. . COMMUNICATION / COORDINATION

Only the TWR and GND ATCO may be expected to work in the same room. If it is assumed that the amount of communication/co-ordination is equal for all combinations of ATCO's, the probabilities as listed in Table 5 can be derived.

ATCO	communication/ co-ordination takes place in the same room (without using telephone/radio)	communication/ co-ordination does not take place in the same room (using telephone/radio)
TWR	0.67	0.33

Table 5 Probability of communication/coordination in the same room.

Next section describes the elicitation of dependence estimates.

2.2 UNCONDITIONAL AND CONDITIONAL RANK CORRELATIONS

The dependence information was obtained from a single expert on April 11th at NLR offices in Amsterdam. The method described in [13] was used. Basically the method consists in asking conditional probabilities of exceedence to experts in order to retrieve the conditional rank correlation required.

In this case the questions asked were roughly the ones presented in Table 6. The expert declared that though heavy traffic would make controllers more concentrated in their job, increases in *traffic* would still increase the proclivity of ATCs to commit human errors (positive dependence) and hence $P_1 > 0.5$. For the second question the expert believed that *experience* would make the probability of ATCo human error reduce and hence $P_2 < P_1$. The fact that the ATC operates with all the equipment required would again decrease the probability of ACT human error and again $P_3 < P_2$ reflecting a negative correlation. If the ATC operates under low visibility procedures the probability of human errors would increase and hence $P_4 > P_3$. Finally the expert believed that given the previous variables the fact that the ATC communicates with other controllers in the same room or by electronic means does not add extra information to the analysis and hence $P_5 = P_4$. Expert's estimates for each conditional probability of exceedence and the corresponding (un)conditional rank correlation retrieved are presented in table 7.

	Probability Asked	Measure Retrieved
$P_1 =$	Probability # ATC errors is above median (5 per million for AL19B8122) Given Traffic (average # aircraft simultaneously under control per hour) is above median (4.1 in this case)	$\rightarrow r_{1,2}$
$P_2 =$	Probability # ATC errors > median Given Traffic > median and # years experience in same position is above median (7.6 years)	$\rightarrow r_{1,3 2}$
$P_3 =$	Probability # ATC errors > median Given Traffic > median and Experience > median and the ATC uses radio, primary, secondary radar and other tools (state 4 probability 80%)	$\rightarrow r_{1,4 2,3}$
$P_4 =$	Probability # ATC errors > median Given Traffic > median and Experience > median and Man Machine Interface = 4 and at least a visibility procedure for BZA is used (state larger than 1 probability 0.05)	$\rightarrow r_{1,5 2,3,4}$
$P_5 =$	Probability # ATC errors > median Given Traffic > median and Experience > median and Man Machine Interface = 4 and Visibility Procedure > 1 and Coordination between ATC is in the same place (Probability = 0.67)	$\rightarrow r_{1,6 2,3,4,5}$

Table 6. Questions asked to expert for dependence elicitation.

Probability Asked		Measure Retrieved	
$P_1 =$	0.75	$\rightarrow r_{6,1} =$	0.69
$P_2 =$	0.625	$\rightarrow r_{6,2 1} =$	-0.52
$P_3 =$	0.572	$\rightarrow r_{6,3 1,2} =$	-0.52
$P_4 =$	0.89	$\rightarrow r_{6,4 1,2,3} =$	0.62
$P_5 =$	0.89	$\rightarrow r_{6,5 1,2,3,4} =$	0.00

Table 7. Results of expert dependence elicitation.

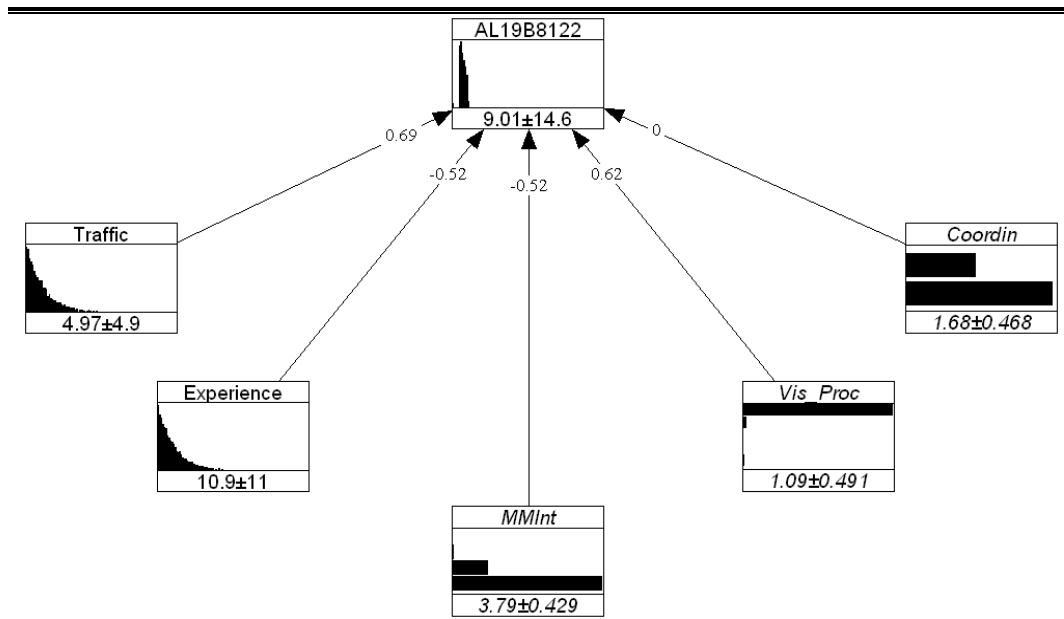


Figure 5. Air Traffic Control Human Performance Model.
(Preliminary Results)

Figure 5 presents the ATC human performance model with its current quantification. If all variables in figure 5 were continuous then the rank correlation matrix of the model would be as in table 8

1	0	0	0	0	0.7069
0	1	0	0	0	-0.3804
0	0	1	0	0	-0.3207
0	0	0	1	0	0.3207
0	0	0	0	1	0
0.7069	-0.3804	-0.3207	0.3207	0	1

Table 8. Rank correlation matrix assuming all variables are continuous.

2.2.1. CONTINUITY CORRECTION.

As explained in [14] one class of distributions can be obtained as monotone transforms of uniform variables. These distributions can be constructed by specifying a marginal distribution and a copula². Consider:

- A population distributed according to two variables X and Y .
- Two independent members of this population (X_1, Y_1) and (X_2, Y_2)
- $(X_1, Y_1) \sim F_{XY}$ with marginals F_X and F_Y and
- $(X_2, Y_2) \sim$ independent with margins F_X and F_Y .

The population version of Spearman's rank correlation is defined as:

$$r = 3 \cdot [P_c - P_d] = 3 \cdot P((X_1 - X_2)(Y_1 - Y_2) > 0) - P((X_1 - X_2)(Y_1 - Y_2) < 0) \quad (1)$$

Where P_c and P_d are the probabilities of concordance and discordance. In order to establish the sample version of equation (1) rank the sates of X_i from 1 to m and those of Y_i from 1 to n

$X_1 \setminus Y_1$	1	2	...	n		$X_2 \setminus Y_2$	1	2	...	n	
1	p_{11}	p_{12}	...	p_{1n}	p_{1+}	1	q_{11}	q_{12}	...	q_{1n}	p_{1+}
2	p_{21}	p_{22}	...	p_{2n}	p_{2+}	2	q_{21}	q_{22}	...	q_{2n}	p_{2+}
...
m	p_{m1}	p_{m2}	...	p_{mn}	p_{m+}	m	q_{m1}	q_{m2}	...	q_{mn}	p_{m+}
	p_{+1}	p_{+2}	...	p_{+n}			p_{+1}	p_{+2}	...	p_{+n}	
	(a)						(b)				

Table 9. (a) Joint distribution of (X_1, Y_1) and (b) Joint distribution of (X_2, Y_2)

In table 9 p_{i+} for $i = 1, \dots, m$ represent the margins for X_1 and X_2 . The margins for Y_1 and Y_2 are denoted p_{+j} for $j = 1, \dots, n$. Since (X_2, Y_2) are independent, then $q_{ij} = p_{i+} p_{+j}$ for all i, j .

$$\tilde{r}_C = \frac{[P_c - P_d]}{\left[\left(\sum_{j>i} p_{i+} p_{+j} - \sum_{k>j>i} p_{i+} p_{+j} p_{+k} \right) \cdot \left(\sum_{j>i} p_{+i} p_{+j} - \sum_{k>j>i} p_{+i} p_{+j} p_{+k} \right) \right]^{1/2}} \quad (2)$$

$$P_c - P_d = \sum_{i=1}^{m-1} \sum_{j=1}^{n-1} (p_{i+} + p_{(i+)+}) (p_{+j} + p_{+(j+)}) C_r \left(\sum_{k=1}^i p_{+k}, \sum_{l=1}^j p_{+l} \right) - \sum_{i=1}^{m-1} \sum_{j=1}^{n-1} p_{i+} p_{+j} \quad (3)$$

The relationship between the rank correlation of the discrete variables \tilde{r}_C and the rank correlation of the underlying uniforms is given by equation (2). In equation (3) C_r is a positively ordered copula parametrized by the rank correlation r . In [14] it is observed that \tilde{r}_C will be an increasing function of the rank correlation in the underlying uniforms (r).

² A copula is a distribution on the unit square with uniform margins. The normal copula is the copula of interest in this application. For a summary on copulas see the appendix.

Since experts were asked about the rank correlation in the underlying uniforms, from figure 8 one can read the corresponding values of the rank correlation in the discrete variates. Table 10 presents the theoretical rank correlation that should be observed from expert's assessments and the correction from figures 8 (a) and (b). Finally table 11 presents the rank correlation matrix obtained by sampling the model in figure 5.

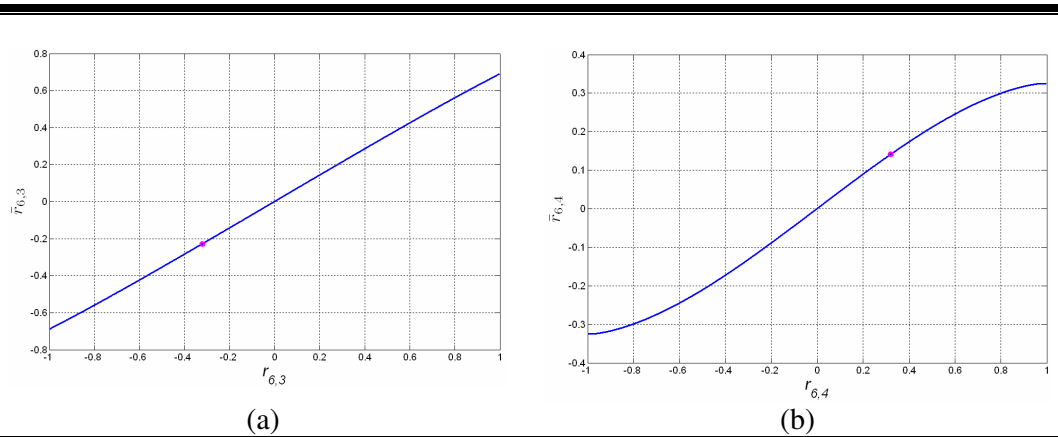


Figure 8. Relationship between rank correlation in the underlying uniforms and the discrete variates.

1	0	0	0	0	0.7069
0	1	0	0	0	-0.3804
0	0	1	0	0	-0.2285
0	0	0	1	0	0.1409
0	0	0	0	1	0
0.7069	-0.3804	-0.2285	0.1409	0	1

Table 10. Theoretical rank correlation matrix of the model in figure 5.

1	-0.0034	0.0041	0.0029	-0.0003	0.6899
-0.0034	1	-0.0006	-0.0004	0.0019	-0.3654
0.0041	-0.0006	1	-0.0002	-0.0009	-0.2193
0.0029	-0.0004	-0.0002	1	-0.0016	0.1402
-0.0003	0.0019	-0.0009	-0.0016	1	-0.0009
0.6899	-0.3654	-0.2193	0.1402	-0.0009	1

Table 11. Sample rank correlation matrix of the model in figure 5.

3. UNIEXP.

The methods employed by UniExp to elicit unconditional and conditional rank correlations from experts are described in [13]. In the appendix to this report, a manual to operate UniExp is included. As explained in [13] the normal copula is chosen to realize the joint distribution in the BBN being elicited. To compute the different probabilities of exceedence in a given BBN as functions of the conditional rank correlations, integrating the multivariate normal density is required. The main focus in this section will be to show discrepancies encountered in two different integration methods used by different versions of UniExp. To observe these differences two models will be used: the flight crew performance model from [6] and the air traffic control error probability model introduced in section 2. Since the purpose of this section is for illustration only, a single expert will be used in the case of flight crew performance and not the combined opinion as in [6].

3.1 FLIGHT CREW ERROR PROBABILITY.

The Flight crew error model introduced in [6] is repeated here for convenience. Table 4 presents the variables considered in the flight crew performance model and the model itself is shown in figure 2.

Index	Name	Description	Source
1	FOExp	Total number of hours flown since the pilot's license obtaining by first officers.	Data
2	FOTraining	Number of days passed since last recurrence training for First Officers.	Data
3	Fatigue	Stanford Sleepiness Scale. 1 signifies "feeling active and vital; wide awake" and 7 stands for "almost in reverie; sleep onset soon; struggle to remain awake".	Data
4	CapTraining	Number of days passed since last recurrence training for Captains.	Data
5	CapExp	Total number of hours flown since the pilot's license obtaining by captains.	Data
6	CapSuit	Number of Captains failing their proficiency check test per 10'000	Expert Judgment
7	FOSuit	Number of First Officers failing their proficiency check test per 10'000	Expert Judgment
8	Weather	Rainfall rate (mm/hr)	Data
9	DLanguage	Number of flights in which the pilot and first officer will have a different mother tongue per 100'000	Expert Judgment
10	CrewSuit	Number of Captains or/and First Officers failing their proficiency check test per 10'000	Expert Judgment
11	AGeneration	Aircraft generation is a scale from 1 to 4 where 4 is the most recent generation of aircrafts	Data
12	Workload	Number of times the crew members have to refer to the abnormal/emergency procedures section of the aircraft operation manual during flight per 100,000 flights	Expert Judgment
13	HError	Number of un recovered errors during any flight phase that might lead to a hazardous situation during the flight per 100,000	Expert Judgment

Table 4. Flight Crew Error Variables.

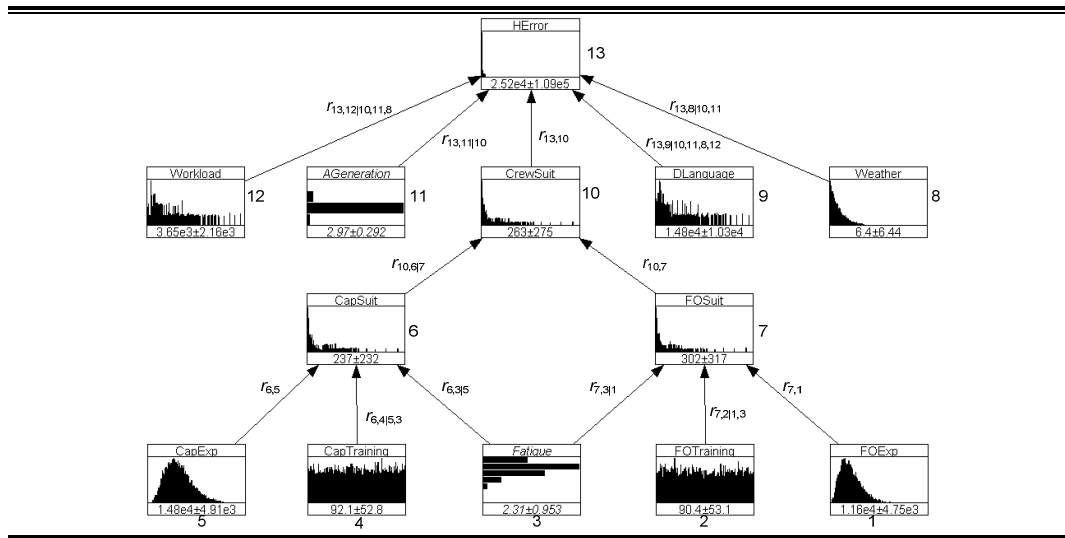


Figure 9. Flight Crew Error Model.
(Preliminary Results)

As explained previously, discrepancies in the algorithms used in the old version of the elicitation software (UniExp) and the latest one to compute the integrals required to compute P_i as a function of the conditional rank correlations were found for $i \geq 3$. For the case of the flight crew error probability model these discrepancies may be observed in Table 2 and Appendix 2. In Table 2, the conditional rank correlations where discrepancies have been found are shaded. In the appendix the whole conditional probability as a function of the conditional rank correlation is shown for the same shaded cases. The reader may observe that the largest differences appear in $r_{13,8|10,11}$ and $r_{13,9|10,11,8,12}$. In the last case differences can be very large.

Rank Correlation	Value (1)	Value (2)	Rank Correlation	Value (1)	Value (2)
$r_{7,1}$	-0.57	-0.57	$r_{10,6 7}$	0.998	0.998
$r_{7,3 1}$	0.19	0.19	$r_{13,10}$	0.57	0.57
$r_{7,2 1,3}$	0.51	0.55	$r_{13,11 10}$	-0.71	-0.71
$r_{6,5}$	-0.3	-0.3	$r_{13,8 10,11}$	0.2	0.271
$r_{6,3 5}$	0.32	0.32	$r_{13,12 10,11,8}$	0.4	0.357
$r_{6,4 5,3}$	0.167	0.15	$r_{13,9 10,11,8,12}$	0.23	0.885
$r_{10,7}$	0.720	0.718			

Table 2. Comparison

Value (1) Corresponds to values computed with UniExp version 1

Value (2) Corresponds to values computed with the current version of UniExp

3.1 AIR TRAFFIC CONTROL ERROR PERFORMANCE MODEL.

As for the Air Traffic Control human performance model, the discrepancies may be observed in figures 10 – 12 for P_3 , P_4 and P_5 . The reader should remember that both algorithms give exactly the same result for P_1 and P_2 . In this case the differences are dramatic from starting from P_3 . In both algorithms conditional independence is captured accurately however P_i as a function of the conditional rank correlation is completely different. Previous calculations performed with the old algorithm should be corrected (see section 3.2).

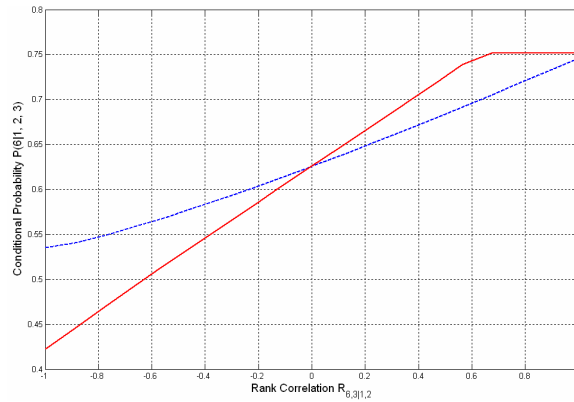


Figure 10. P_3 as a function of $r_{\theta,3|1,2}$ for two different integration algorithms. The dashed line corresponds to the current more accurate algorithm.

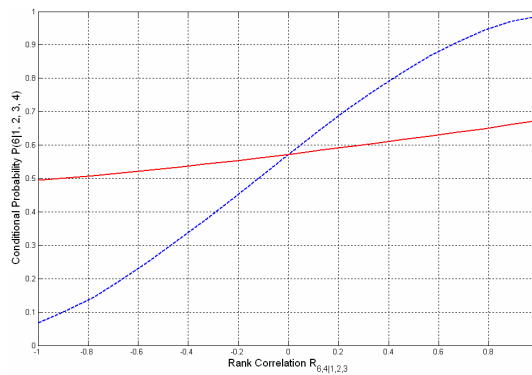


Figure 11. P_4 as a function of $r_{\theta,4|1,2,3}$ for two different integration algorithms. The dashed line corresponds to the current more accurate algorithm.

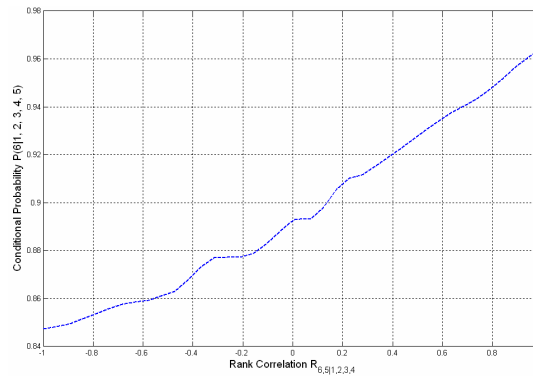


Figure 12. P_5 as a function of $r_{0, 5|1, 2, 3, 4}$ computed with the current more accurate algorithm.

In figure 12 only the current's algorithm result is presented since the bounds for P_5 would fall outside the expert's assessment if computed with the old algorithm.

4. FUTURE WORK.

Future work from the EWI-TU Delft group includes:

1. Finalize the quantification of the BBN ATC human performance. This will be done in combination with NLR and with the cooperation of experts.
2. Support the construction of new models for other parts of the CATS 'back bone' model.
3. Continue assembling a single Bayesian Network from FTs, ESDs and continuous BBNs.
4. Continue enhancing the software tools for elicitation and construction of BBNs.

Further work to be performed as agreed on the technical meetings.

BASIC BIBLIOGRAPHY.

- [1] Hanea A.M. et al., “*Hybrid Methods for Quantifying and Analyzing Bayesian Belief Nets*”, Proceedings of the 2005 ENBIS5 Conference, 2005.
- [2] Roelen A.L.C. et al., “*Causal Modelling of Air Safety. Demonstration Model.*” National Aerospace Laboratory, NLR-CR-2002-662, December 2002.
- [3] Cooke R.M. et. al, “*Report on Phase 1 Causal Modeling for Schiphol Airport*”, in Causal Model for Air Transport Safety (CATS). Third Interim report. 4 February 2006. Risk Centre TU Delft.
- [4] Morales O. et. al, “*Report on Phase 2 Causal Modeling for Schiphol Airport*”, in Causal Model for Air Transport Safety (CATS). Fourth Interim report. 4 May 2006. Risk Centre TU Delft.
- [5] Cooke R.M. “*Experts in Uncertainty: Opinion and Subjective Probability in Science*” in Environmental Ethics and Science Policy Series, Oxford University Press, June 1991.
- [6] Morales O. et. al, “*Report on Phase 3 Causal Modeling for Schiphol Airport*”, in Causal Model for Air Transport Safety (CATS). Fifth Interim report. 4 May 2006. Risk Centre TU Delft.
- [7] Bobbio A. et. al, “*Improving the Analysis of Dependable Systems by Mapping fault trees into Bayesian Networks*”, Reliability Engineering & System Safety 71 (2001), 249-260.
- [8] Bedford T. & Cooke R.M. “*Mathematical Tools for Probabilistic Risk Analysis*” Cambridge University Press, 2001.
- [9] Ale B.J.M. “*Causal Model for Air Transport Safety: Fifth Interim Report*” August 1 2006. Risk Centre TU Delft.
- [10] Morales O. et. al, “*Report on Phase 4 Causal Modeling for Schiphol Airport*”, in Causal Model for Air Transport Safety (CATS).
- [11] Roelen A.L.C. et al., “*Quantification of Event Sequence Diagrams for Causal risk Model of Commercial Air Transport*” National Aerospace Laboratory, NLR-CR-2006-520.
- [12] Morales O. et. al, “*Report on Phase 5 Causal Modeling for Schiphol Airport*”, in Causal Model for Air Transport Safety (CATS).
- [13] Morales O. et. al, “*Eliciting conditional and unconditional rank correlations from conditional probabilities*”, Reliability Engineering and System Safety (2007), <http://dx.doi.org/10.1016/j.res.2007.03.020>

[14] Hanea A. M et al, "*The population version of Spearman's rank correlation coefficient in the case of ordinal discrete random variables*", Proceedings of the Third Brazilian Conference on Statistical Modelling in Insurance and Finance.

APPENDIX 1 AIR TRAFFIC CONTROL ERRORS IN FTs

Error	Name of Variable	Probability	Description
ATC delay	TO06B3.3.1	3.34E-05	The probability has been calculated using the relevant pivotal event probability (Section 8 NLR Report) and the casual failure distribution and method in Appendix II Section 6.4.1 Referenced DNV report
ATC delay	TO06B2.3.1	9.99E-04	The probability has been calculated using the relevant pivotal event probability (Section 8 NLR Report) and the casual failure distribution and method in Appendix II Section 6.4.1 Referenced DNV report
ATC fail to advise pilot	TO08B1.1.3	2.57E-02	As the DNV probabilities (Appendix II Section 8.4.1 Referenced DNV report) were based upon judgements they have been adjusted using the relevant pivotal event probability (Section 10 NLR Report) to reflect the difference in the NLR & DNV pivotal event probability "Flight Crew fails to detect windshear"
Aircraft diverted from other location	AL19B8.1.2.2	6.64E-06	The documentation of this base event is to updated
Failure of ATC to advise pilot	AL23B1.1.3	1.50E-01	As the DNV probabilities (Appendix II Section 8.4.1 Referenced DNV LOC-TO report) were based upon judgements they have been adjusted using the relevant pivotal event probability (Section 23 NLR Report) to reflect the difference in the NLR & DNV pivotal event probability "Flight Crew fails to detect windshear"
ATC fail to report weather to pilot	AL30B2.1.1	3.06E-04	The probability has been calculated using causal distibution taken from accident data, the probability of severe wind condition sin the fault tree and the pivotal event probability, AL30a1 taken from Section 29 of NLR report
Weather not as reported by MET Services	AL30B2.1.2	3.06E-04	The probability has been calculated using causal distibution taken from accident data, the probability of severe wind condition sin the fault tree and the pivotal event probability, AL30a1 taken from Section 29 of NLR report
Unsuccessful ATCO monitoring of TAR	AL35B321	3.72E-01	The probability, given a CFTT incident with TAR available, that the controller (ATCO) fails to detect the CFTT in time to be able to prevent an imminent CFIT.

ATCO failure to respond to MSAW warning	AL35B3223	2.00E-01	The probability, given a CFTT incident with MSAW warning, that the ATCO does not respond in time to be able to prevent an imminent CFIT.
ATCO failure to resolve conflict in time	AL35B33	1.00E-01	The probability, given a CFTT incident with ATCO alerted by an MSAW warning, that the ATCO and flight crew do not correct CFTT in time to prevent an imminent CFIT.
Incorrect clearance causes ITC	AL35F5214	2.44E-05	The probability, given a manual trajectory command during approach, of ITC due to incorrect ATC clearances. This only covers cases where incorrect clearances directly cause the pilot to command flight towards terrain.
Inadequate trajectory command by ATCO (ITC)	AL35F721	3.64E-04	The probability, given an ATC trajectory command during approach, of ITC due to errors by the ATCO.

APPENDIX 2 DISCREPANCIES BETWEEN TWO DIFFERENT ALGORITHMS TO INTEGRATE THE MULTIVARIATE NORMAL DENSITY FUNCTION

FLIGHT CREW ERROR PROBABILITY MODEL

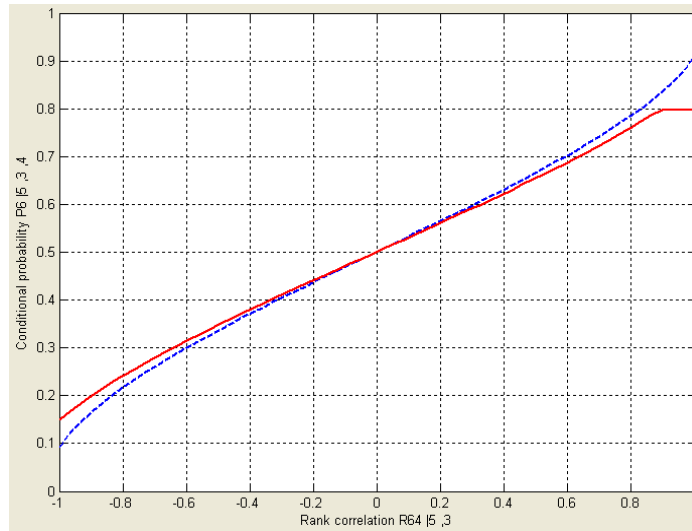


Figure A2.1 $P_{6|5,3,4}$ as a function of $r_{6,4|5,3}$ for two different integration algorithms. The dashed line corresponds to the current more accurate algorithm.

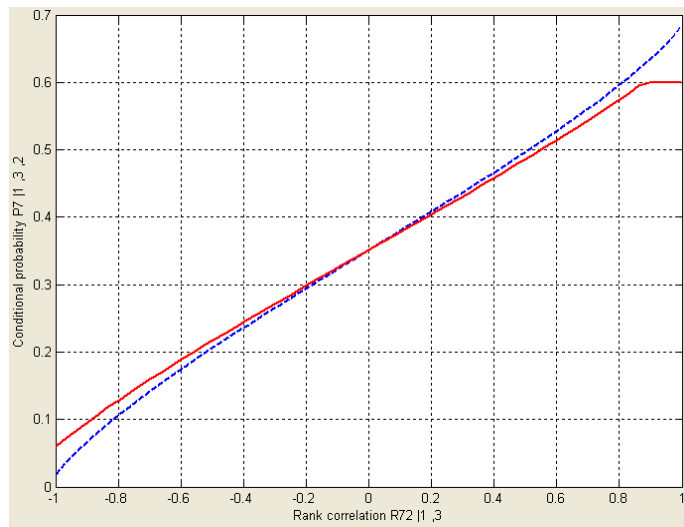


Figure A2.2 $P_{7|1,3,2}$ as a function of $r_{7,2|1,3}$ for two different integration algorithms. The dashed line corresponds to the current more accurate algorithm.

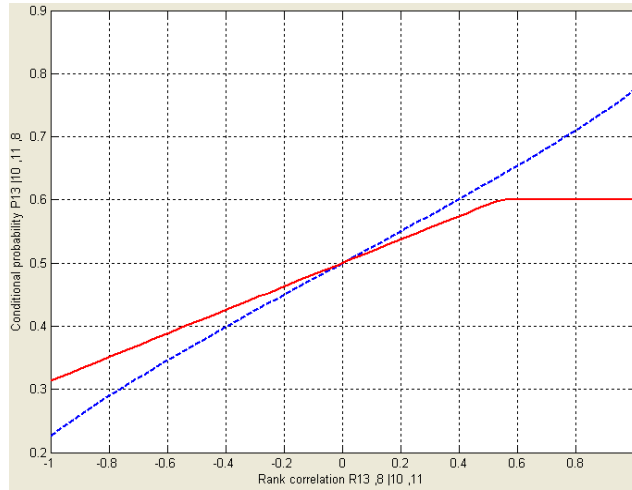


Figure A2.3 $P_{13|10,11,8}$ as a function of $r_{13,8|10,11}$ for two different integration algorithms. The dashed line corresponds to the current more accurate algorithm.

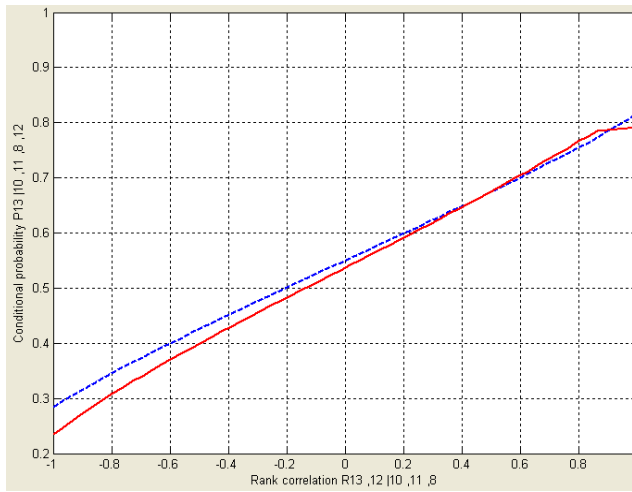


Figure A2.4 $P_{13|10,11,8,12}$ as a function of $r_{13,12|10,11,8}$ for two different integration algorithms. The dashed line corresponds to the current more accurate algorithm.

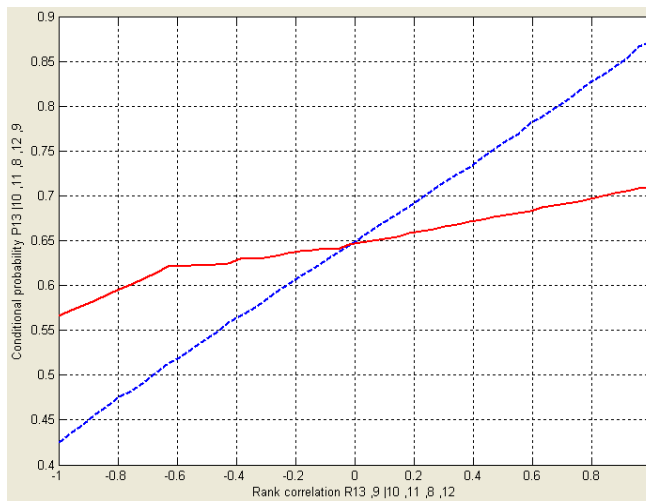


Figure A2.5 $P_{13|10,11,8,12,9}$ as a function of $r_{13,12|10,11,8,9}$ for two different integration algorithms. The dashed line corresponds to the current more accurate algorithm.